

Hepatitis Delta Virus Antigen Forms Dimers and Multimeric Complexes In Vivo

JIA-GANG WANG^{1,2} AND STANLEY M. LEMON^{1*}

Departments of Medicine¹ and Epidemiology,² The University of North Carolina at Chapel Hill, Chapel Hill, North Carolina 27599-7030

Received 8 June 1992/Accepted 22 September 1992

Although the hepatitis delta virus genome contains multiple open reading frames, only one of these reading frames is known to be expressed during replication of the virus. This open reading frame encodes two distinct molecular species of hepatitis delta antigen (HDAg), p24^s and p27^s, depending on the location of the stop codon which terminates translation. We found antibody specific for p27^s to be capable of precipitating p24^s in extracts of infected liver, indicating that p27^s and p24^s form heterologous complexes in vivo. After cross-linking with 0.05% glutaraldehyde, specific HDAg dimers were detected in antigen prepared from both the liver and serum of an HDV-infected woodchuck carrier of woodchuck hepatitis virus. Guanidine HCl-denatured HDAg extracted from liver and dialyzed against phosphate-buffered saline sedimented in rate-zonal sucrose density gradients as 15S multimeric complexes. These 15S multimers were stable in the presence of 1.2% Nonidet P-40. After RNase digestion, the 15S complex was reduced to a 12S complex without associated RNA, while boiling for 3 min in 1% sodium dodecyl sulfate-0.5% 2-mercaptoethanol further reduced the 15S complex to 3S HDAg monomers. In the absence of glutaraldehyde cross-linking, HDAg extracted from liver migrated as monomer species in reducing and nonreducing gels, suggesting that the conserved cysteine residue present in p27^s does not play a role in the formation of either dimers or multimers. On the other hand, an amino-terminal chymotrypsin-digested HDAg fragment, with a predicted length of 81 or less amino acids, retained the ability to form dimers, consistent with the hypothesis that a coiled-coil motif present between residues 27 and 58 may play a role in HDAg protein interactions in vivo.

Hepatitis delta virus (HDV) is a defective satellite virus which is capable of replication only in the presence of a coinfecting hepadnavirus such as hepatitis B virus (14, 17-19). The HDV particle is 36 nm in diameter and contains a circular single-stranded RNA genome of about 1,680 bases in length in association with two closely related viral proteins, p24^s and p27^s (7, 12, 24, 25). Although multiple open reading frames (ORFs) are present within the sequences of both genomic and antigenomic HDV RNAs, these two molecular forms of the hepatitis delta antigen (HDAg) are encoded by the same ORF and represent the only viral proteins known to be expressed during virus replication (22, 26). p27^s differs from p24^s in having a 19-residue carboxy-terminal extension and is encoded by RNAs in which UAG (termination) at codon 196 of this ORF has undergone mutation to UGG (Trp) (10). Available evidence suggests that p24^s is necessary for replication of HDV RNA, while p27^s down-regulates RNA replication and may specifically mediate HDV particle assembly (3, 5, 20, 21). Only viral RNAs encoding p24^s appear to be infectious, but mutation at codon 196 with subsequent expression of p27^s occurs regularly during HDV replication and may be an important regulatory mechanism (10).

The mechanism by which p24^s supports replication of the viral RNA remains unclear, although it may play an important role in directing transport of the viral RNA to the nucleus where replication occurs (27). Previous work examining the stoichiometry of the dominant negative regulatory effect of p27^s on RNA replication suggests that p27^s might function as part of a multimeric complex, as p27^s was able to exert a down-regulating effect even when p24^s was present in

a 20-fold molar excess (5). This hypothesis is further supported by the demonstration that polypeptides expressed from segments of the HDAg ORF in vitro were capable of forming dimers (8). In this report, we present data that indicate that HDAg is naturally present as dimers in vivo and that specific multimeric aggregates of HDAg assemble after removal of guanidine HCl from crude, nonpurified, denatured liver-derived antigen. Furthermore, we show that dimerization of HDAg is mediated through the amino-terminal 81 residues of this protein, which contain a conserved coiled-coil structural motif.

MATERIALS AND METHODS

Anti-HDV sera. Human anti-HDV serum was collected from a patient with classical hemophilia and chronic HDV infection. Antipeptide antisera were collected from guinea pigs and rabbits immunized with synthetic peptides corresponding to various segments of the large HDAg molecule (Makino sequence 12) (Table 1). For use in immunization, these peptides were conjugated to keyhole limpet hemocyanin as described previously (22).

HDAg. Liver and serum were collected from a woodchuck carrier of the woodchuck hepatitis virus which was experimentally infected with HDV in collaboration with John Cullen of the College of Veterinary Medicine, North Carolina State University. For extraction of HDAg from infected woodchuck liver under denaturing conditions, 1 g of liver tissue was homogenized in 3 ml of 6 M guanidine-HCl and then dialyzed against phosphate-buffered saline (PBS) overnight at 4°C (2). After centrifugation at 2,000 × g for 20 min, the supernatant was stored in aliquots at -70°C. This procedure does not result in purification of the HDAg from other liver proteins. Serum (1.0 ml) taken from an acutely

* Corresponding author.

TABLE 1. Synthetic HDAg peptides used for production of anti-peptide antibodies^a

Peptide	HDag residues	Sequence
D5/58-78	58-78	C-IGKKDKDGE GAPPAAKKLRMDQ
D5/82-102	82-102	C-DAGPKRPLRGGF TDKERQDH
D5/123-143	123-143	C-SREFFEEELKRLTEDEKERRR
D5/156-184	156-184	C-EGGSDGAPGGGFVPSMQGVGPSFARTGE
D5/197-211	197-211	DILFPADPPFPSPQSC

^a See also reference 22.

superinfected woodchuck (WC 643) was layered over an 11-ml cushion containing 20% sucrose in 0.02 M HEPES (*N*-2-hydroxyethylpiperazine-*N'*-2-ethanesulfonic acid) (pH 7.4)–0.01 M CaCl₂–0.01 M MgCl₂–0.1% bovine serum albumin and centrifuged for 5 h at 15,000 × *g* in an SW40 rotor. Pelleted HDag was resuspended in distilled water and stored at –70°C until use.

Immunoprecipitation of HDag. HDag derived from woodchuck liver was preincubated with protein A-Sepharose (Sigma) for 30 min at 4°C and then centrifuged for 5 min at 14,000 rpm in an Eppendorf microcentrifuge. The supernatant fluid (50 µl) was incubated for 60 min at 4°C with 7 µl of rabbit anti-peptide serum diluted 1:100 in NTE buffer (50 mM Tris-HCl [pH 7.5], 150 mM NaCl, 0.1% Nonidet P-40 [NP-40], 1 mM EDTA, 0.25% gelatin, 0.02% sodium azide). Protein A-Sepharose (8 mg in 750 µl) was added to the antigen-antibody mixtures, and the incubation continued for 60 min at 4°C with agitation. The tertiary HDag-antibody-protein A-Sepharose complex was pelleted by centrifugation for 5 min in the microcentrifuge. The pellets were washed three times in washing buffer (10 mM Tris-HCl, 0.1% NP-40) for 10 min with gentle agitation. Pelleted complexes were resuspended in distilled water and stored at –70°C until sodium dodecyl sulfate-polyacrylamide gel electrophoresis (SDS-PAGE) and immunoblot analysis.

Rate-zonal centrifugation of HDag complexes. Linear sucrose density gradients (10 to 30% [wt/vol]) were prepared in a buffer containing 20 mM Tris-HCl (pH 7.4), 150 mM NaCl, and 1 mM EDTA. HDag (100 µl) extracted from liver tissue was mixed with 30 µl of human anti-HDag-negative serum containing marker immunoglobulins and loaded on the top of the gradient before centrifugation for 18 h at 35,000 rpm in an SW41 rotor. Fractions were collected from the bottom of the gradients and tested for HDag by radioimmunoassay or by SDS-PAGE followed by immunoblotting.

Glutaraldehyde cross-linkage of HDag. HDag was cross-linked by treatment with 0.04 or 0.05% glutaraldehyde for 2 or 5 min. Antigen extracted from infected woodchuck liver was directly cross-linked, while HDag derived from serum was incubated with 0.3% NP-40 overnight at 4°C before treatment with glutaraldehyde. Cross-linkage was stopped by the addition of an equal volume of 2× Laemmli sample buffer (0.125 M Tris-HCl [pH 6.8] 2% SDS, 10% glycerol, 1% 2-mercaptoethanol). After boiling for 5 min, the cross-linked proteins were separated by 12 or 15% PAGE-SDS and transferred to either nitrocellulose paper or Immobilon-p transfer membranes (Millipore) for immunoblot analysis.

Chymotrypsin digestion of HDag. Liver-derived HDag was digested with various concentrations of chymotrypsin in PBS for 30 min at 37°C. Digestion was stopped by adding an equal volume of 2× Laemmli buffer and then boiling for 5 min.

Detection of HDag by radioimmunoassay. HDag was

detected by a microtiter solid-phase radioimmunoassay modified from that described by Rizzetto et al. (19). Flexible polyvinyl chloride microtiter plate wells were coated for 2 h at 37°C with 100 µl of a human anti-HDag-positive serum (AM084) diluted 1:4,000 in 50 mM carbonate buffer (pH 9.6), washed with PBS containing 0.05% Tween 20 (PBS-T), and loaded with 60 µl of test material (sucrose gradient fractions diluted 1:2 in PBS containing 10% fetal calf serum). After incubation overnight at room temperature, the plates were rewashed with PBS-T and incubated for 4 h at 4°C with 60 µl of ¹²⁵I-labelled immunoglobulin G (IgG) (50,000 cpm) (23). After further washing, the individual wells were cut from the plate, and bound radioactivity was measured in an automatic gamma scintillation counter.

Immunoblot detection of HDag. Immunoblot detection of HDag was done similarly to the method described previously (23). In brief, proteins blotted onto nitrocellulose paper or Immobilon-p transfer membranes were blocked with 5% nonfat milk in PBS for 60 min and then incubated with primary antibody (human convalescent anti-HDag-positive antisera or guinea pig or rabbit anti-peptide antisera diluted 1:250 to 1:1,000) for 1 h at room temperature. After three washes in PBS, blots were incubated with a horseradish peroxidase-conjugated anti-immunoglobulin antibody, and then washed with PBS. Blots were then either incubated in TMB (3,3',5,5'-tetramethylbenzidine) substrate buffer or processed for detection of horseradish peroxidase by enhanced chemiluminescence (ECL Western immunoblotting detection system; Amersham). Antibodies bound to blots analyzed with the ECL system were removed by incubation in stripping buffer (100 mM 2-mercaptoethanol, 2% SDS, 62.5 mM Tris-HCl [pH 6.7]) for 30 min at 60°C with occasional agitation. Blots were then washed twice in PBS-T for 10 min at room temperature and reprobed with an alternative primary antibody as described above.

HDV RNA detection. HDV RNA was detected in gradient fractions by slot-blot hybridization with probes consisting of genomic- and antigenomic-sense synthetic RNAs (bases 486 to 1426) transcribed from the plasmid pGEM⁸. pGEM⁸ contains the small *Eco*RI fragment of pδ4 (24) ligated into the multiple cloning site of pGEM-3Zf(+) (Promega). For preparation of RNA probes, pGEM⁸ was linearized by either *Sac*I (genomic sense) or *Apa*I (antigenomic sense), and the 3' overhangs were repaired with the Klenow fragment of *Escherichia coli* DNA polymerase. Runoff ³²P-labelled RNA transcripts were synthesized under direction of T7 (genomic sense) or SP6 (antigenomic sense) RNA polymerases by standard protocols (Promega). For preparation of blots, aliquots (30 µl) of sucrose gradient fractions were incubated with 150 µl of lysing buffer (0.2 M NaCl, 2.0% SDS, 50 mM Tris [pH 7.4], with proteinase K [50 µg/ml] and RNasin [500 U/ml]) for 30 min at 37°C and added to 250 µl of blotting buffer (14% formaldehyde, 7.5× SSC [1× SSC is 0.15 M NaCl plus 0.015 M sodium citrate]). The mixture was brought to 65°C for 45 min before vacuum blotting onto nitrocellulose paper. Blots were baked for 2 h at 80°C and prehybridized for 4 h at 60°C in a buffer containing 40% formamide, 5× SSC, 0.05 M sodium phosphate (pH 6.5), 0.01% SDS, and 8× Denhardt's solution, as described by Negro et al. (13). Hybridization was done at 60°C for 12 h in the same buffer containing RNA probes at a concentration of 2 × 10⁶ cpm/ml. Blots were subsequently washed three times in 400 ml of high-salt washing buffer (2× SSC, 0.1% SDS) at room temperature and once at 75°C; this was followed by three washes in 400 ml of low-salt buffer (0.1× SSC, 0.1% SDS) at 75°C (15 min per wash). Autoradiographic (Kodak

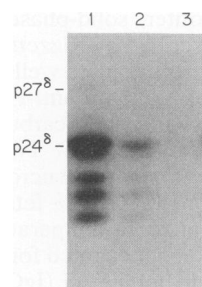


FIG. 1. Immunoprecipitation of HDAG present in liver extracts with rabbit antibodies to synthetic HDAG peptides. Immunoprecipitated HDAG was separated by SDS-PAGE, transferred to nitrocellulose paper, and detected with radiolabelled polyclonal human anti-HDAG antibodies. Antipeptide antibodies were D5/156-184 (lane 1), D5/197-211 (lane 2), or an unrelated hepatitis A virus peptide (lane 3).

XAR-5 film) exposure was for 15 h at -70°C with an intensifying screen.

PEPSCAN analysis of antipeptide antibodies. Overlapping hexapeptides spanning the entire HDAG molecule were synthesized on polyethylene pins with materials purchased from Cambridge Research Biochemicals, Inc. (Valley Stream, N.Y.) as previously described (23). Oligopeptide-bearing pins were blocked by incubation for 1 h at room temperature in microtiter plates containing 200 μl of blocking buffer (1% ovalbumin, 1% bovine serum albumin, 1% Tween 20 in PBS) per well. Pins were then transferred to a microtiter plate containing 175 μl per well of guinea pig antipeptide serum diluted 1:1,000 in blocking buffer. After incubation at 4°C for 18 h, pins were subjected to three cycles of washing in PBS-T (10 min per cycle with agitation), transferred to wells containing horseradish peroxidase-conjugated rabbit anti-guinea pig immunoglobulins (Dako) diluted 1:2,000 in blocking buffer, and incubated for 60 min at room temperature. After further washing steps, pins were placed in microtiter wells containing 150 μl of freshly prepared substrate solution (23) and held at room temperature in the dark for 30 min. Color development was stopped by removal of the pins, and the A_{405} was determined immediately in an automated enzyme-linked immunosorbent assay plate reader.

RESULTS

Immunoprecipitation of HDAG with antipeptide antisera.

We previously demonstrated that antisera raised in guinea pigs to a peptide representing residues 156 to 184 (peptide D5/156-184 [Table 1]) recognized both small ($p24^{\delta}$) and large ($p27^{\delta}$) forms of HDAG in immunoblots of antigen extracted from infected woodchuck liver. In contrast, antisera raised against a synthetic peptide representing residues 197 to 211 of the large HDAG ORF (peptide D5/197-211) recognized only $p27^{\delta}$ (22). This finding is consistent with the expression of $p27^{\delta}$ occurring as a result of mutation of codon 196 from UAG to UGG (10). However, although anti-D5/197-211 reacted only with $p27^{\delta}$ in immunoblots, $p24^{\delta}$ was the predominant species of HDAG present in liver extracts that was precipitated by this antibody in immunoprecipitation experiments (Fig. 1). Smaller, carboxy-terminally truncated HDAG (22) species were also precipitated. This finding indicates that $p27^{\delta}$ forms heterologous complexes with $p24^{\delta}$ as well as smaller species of HDAG (22) present in antigen

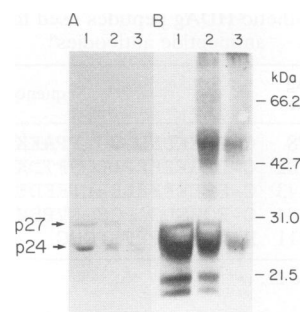


FIG. 2. Immunoblot analysis of glutaraldehyde cross-linked HDAG. The source of HDAG in panel A was HDV-infected woodchuck serum, while the source of HDAG in panel B was woodchuck liver. In each panel, lane 1 contains control antigen which was not cross-linked with glutaraldehyde. Other lanes were loaded with HDAG treated with 0.05% glutaraldehyde for 2 min (lane 2) or 5 min (lane 3). Cross-linking reactions were stopped by the addition of an equal volume of $2\times$ Laemmli sample buffer and then boiling for 5 min before SDS-12% PAGE and subsequent transfer to nitrocellulose paper. HDAG was detected with radiolabelled human polyclonal anti-HDAG.

extracted from infected woodchuck liver under denaturing-renaturing conditions.

Detection of HDAG dimers in woodchuck liver and serum.

To demonstrate the presence of dimeric HDAG, we subjected nonpurified antigens extracted from the liver and serum of infected woodchucks to cross-linking by glutaraldehyde and then SDS-PAGE and transfer to nitrocellulose paper for immunoblot analysis (Fig. 2). After either a 2- or 5-min exposure to glutaraldehyde, the intensity of both $p24^{\delta}$ and $p27^{\delta}$ bands in lanes containing serum-derived HDAG was reduced, and a new HDAG band, migrating with an approximate molecular mass of 43 kDa, became evident (Fig. 2A, lanes 2 and 3). A similar pattern was noted in lanes containing antigen extracted from woodchuck liver (Fig. 2B, lanes 2 and 3). As the serum and particularly the liver-derived antigens analyzed in Fig. 2 were crude preparations containing many host proteins, the presence of high-molecular-weight cross-linked forms of relatively discrete size is indicative of the presence of specific complexes. Although there is a difference in the intensity of the blots shown in Fig. 2A and B, the high-molecular-weight cross-linked HDAG products derived from liver appeared to form a somewhat broader band in SDS-PAGE (Fig. 2B, lane 2 and 3). This suggests a degree of heterogeneity in the size of cross-linked liver-derived HDAG molecules, which would be consistent with the results of immunoprecipitation studies which indicated that $p27^{\delta}$ forms heterologous complexes with $p24^{\delta}$ and other smaller antigen species (Fig. 1). These data thus indicate that HDAG is present as dimers *in vivo* and that these dimers are present in circulating virus particles, as well as in extracts of infected liver tissue which has been subjected to denaturation-renaturation.

Detection of specific multimeric HDAG aggregates. To determine whether HDAG forms larger, multimeric aggregates, we subjected the liver-derived antigen to rate-zonal ultracentrifugation through linear 10 to 30% sucrose density gradients (Fig. 3). HDAG was detected in gradient fractions by a solid-phase radioimmunoassay utilizing ^{125}I -labelled human polyclonal IgG anti-HDAG as a detector antibody. The sedimentation coefficient of HDAG was estimated by comparison with the sedimentation of 19S IgM and 7S IgG

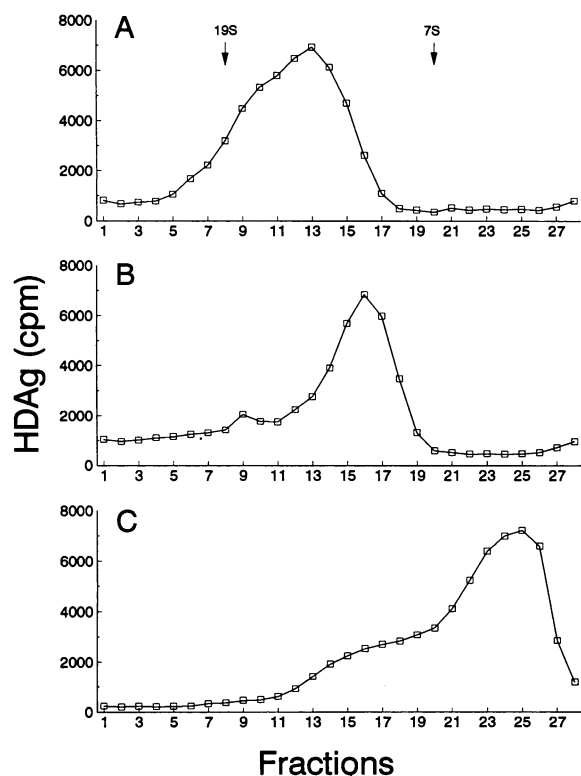


FIG. 3. Rate-zonal 10 to 30% linear sucrose gradients containing HDAg extracted from liver tissue in the presence of 4.5 M guanidine HCl and then dialyzed against PBS. Each gradient was centrifuged for 18 h at 35,000 rpm in an SW41 rotor. Fractions were collected from the bottom of the gradient and tested for HDAg by radioimmunoassay. (A) Gradient loaded with HDAg; (B) parallel gradient in which the HDAg was digested with RNase A before centrifugation; (C) third gradient loaded with HDAg which had been boiled for 5 min in Laemmli sample buffer. Arrows show the position of 19S IgM and 7S IgG within these gradients.

markers present in the same gradient. Under these conditions, the sedimentation coefficient of the major HDAg peak was approximately 15S (Fig. 3A). Because HDAg is known to have RNA binding properties (4, 9), we considered the possibility that this relatively high sedimentation rate might have been due to the association of HDAg with RNA. To evaluate this possibility, liver-derived HDAg was digested with RNase A (10 U/ml for 30 min at 30°C) before rate-zonal centrifugation (Fig. 3B). After RNase treatment, the sedimentation coefficient of the major HDAg was significantly lower (approximately 12S), but still much higher than that expected for monomer HDAg. Thus, the high-molecular-weight 15S HDAg aggregates were associated with RNA, but removal of the RNA by RNase digestion resulted in only a minimal decrease in the sedimentation velocity of HDAg in sucrose gradients. Similar experiments demonstrated that the high-molecular-weight 15S HDAg complex was stable in the presence of 0.6 or 1.2% NP-40 (data not shown). To determine the sedimentation rate of HDAg monomers, the liver-derived HDAg was boiled for 5 min in Laemmli sample buffer before rate-zonal centrifugation. Under these conditions, the peak HDAg activity had a sedimentation coefficient of approximately 3S (Fig. 3C).

When fractions from the sucrose gradient shown in Fig. 3B were subjected to SDS-PAGE and silver staining, numer-

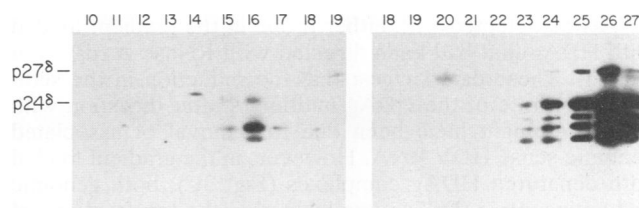


FIG. 4. Immunoblot analysis of HDAg present in fractions of a sucrose gradient loaded with RNase A-digested HDAg (fractions 10 to 19 of the gradient shown in Fig. 3B) (left panel) and a parallel gradient containing HDAg boiled for 5 min in Laemmli sample buffer (fractions 18 to 27 of the gradient shown in Fig. 3C) (right panel). HDAg was detected with a mixture of guinea pig anti-D5/58-78, anti-D5/82-102, and anti-D5/123-143 antibodies; this was followed by application of a peroxidase-conjugated, anti-immunoglobulin antibody which was detected by an enhanced chemiluminescence system.

ous host cell proteins were present in fractions 21 to 28, but no protein bands were observed in fractions below fraction 20 (data not shown). These data suggest that the high-molecular-weight 12S HDAg which was present in fractions 12 to 18 of this gradient represents specific HDAg multimers. Selected fractions from the gradients shown in Fig. 3B and C were subjected to SDS-PAGE and then immunoblot detection of HDAg with enhanced chemiluminescence (Fig. 4). Although p24⁸ was present in the 12S multimeric HDAg complexes, the results of these experiments indicated that the dominant species of HDAg in the complexes was one of about 22.5 kDa. This small HDAg species corresponds to a carboxy-terminally truncated molecule terminating between residues 156 and 170, which is present in the nonpurified liver extract (22).

Virion RNA associated with HDAg multimeric complexes.

The shift in the location of multimeric HDAg within sucrose gradients after digestion with RNase A indicated that the multimers were associated with RNA (Fig. 3A and B). To determine whether this RNA might be related to HDV RNA, we subjected fractions from the gradients shown in Fig. 3A and B to slot-blot hybridization with probes which were specific for genomic or antigenomic strands of HDV RNA. Autoradiograms of these blots were analyzed in a laser densitometer (Fig. 5). In the gradient loaded with undigested HDAg (Fig. 3A), genomic HDV RNA was found to cosediment with multimeric complexes of HDAg (Fig. 5). In contrast, antigenomic RNA was present in the greatest concentrations near the bottom of the gradient. No HDV

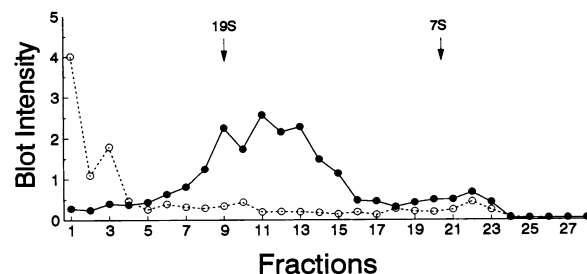


FIG. 5. Genomic (●—●) and antigenomic (○---○) HDV RNA present in fractions from the gradient shown in Fig. 3A. The results shown represent laser densitometry readings of autoradiograms of RNA-RNA slot-blot hybridizations, done on separate blots with strand-specific probes.

RNA was detected with either probe in the gradient loaded with HDaG that had been digested with RNase A (data not shown). These data suggest that the reduction in the sedimentation rate of the HDaG multimers after digestion with RNase A might have been due to removal of associated genomic-sense HDV RNA. However, in the gradient loaded with denatured HDaG complexes (Fig. 3C), both genomic and antigenomic RNAs were located in the top fractions of the gradient, suggesting that the RNA was largely degraded. Consistent with this interpretation, attempts to further characterize the RNA by Northern (RNA) analysis failed to identify a specific RNA band (data not shown).

HDaG multimers assemble after removal of guanidine HCl by dialysis. Because the HDaG that we studied in these experiments was extracted from liver tissue under denaturing conditions, we suspected that the multimeric complexes demonstrated in the rate-zonal sucrose gradients might have assembled during removal of the guanidine by dialysis against a nondenaturing buffer. Alternatively, HDaG complexes present in the liver might have resisted denaturation in 4.5 M guanidine. To distinguish between these two possibilities, a liver homogenate prepared in guanidine was loaded directly onto a sucrose gradient containing 4 M guanidine. A parallel gradient was loaded with HDaG monomers prepared by boiling the liver extract for 8 min in Laemmli sample buffer. Gradients were centrifuged for 21 h, and individual gradient fractions were dialyzed overnight against PBS before assay for HDaG by radioimmunoassay. HDaG in both gradients demonstrated a sedimentation rate characteristic of monomer HDaG (data not shown). Dialysis of the liver extract against PBS before rate-zonal centrifugation resulted in the presence of multimeric complexes similar to those shown in Fig. 3 (data not shown). Thus, large HDaG multimers are unstable in the presence of guanidine and assemble after the removal of guanidine by dialysis.

Role of disulfide bonds in formation of multimeric HDaG complexes. Available sequences of the HDaG ORF show the presence of a single conserved Cys residue, Cys-211, at position 4 from the carboxy terminus of p27⁸. To ascertain whether disulfide bonds involving this Cys residue might play a role in forming multimers or dimers, we performed immunoblots of liver-derived antigen after separation by SDS-PAGE under reducing (1% 2-mercaptoethanol) or nonreducing conditions. The migration of p27⁸ was similar under both conditions, suggesting that disulfide bonds are not important for formation of the multimeric HDaG complex (data not shown). This is consistent with recently published evidence that Cys-211 is prenylated (6).

Partial localization of an HDaG dimerization domain. Guanidine HCl-denatured HDaG, extracted from infected woodchuck liver and dialyzed against PBS, is sensitive to digestion with chymotrypsin (Fig. 6). Digestion with increasing concentrations of the protease for 30 min at 37°C resulted in progressively smaller digestion products. At the minimum effective chymotrypsin concentration (5 µg/ml), multiple HDaG species of different size were reduced to a single unique HDaG polypeptide having an apparent molecular mass of 12.5 kDa and reacting with antibodies to peptide D5/58-78 (Fig. 6, lane 2) and peptide D5/82-102 (data not shown) (Table 1). With increased concentrations of chymotrypsin (50 and 500 µg/ml), this polypeptide fragment was further digested to progressively smaller polypeptides (apparent molecular masses of approximately 10.5 and 10.0 kDa) (Fig. 6, lanes 3 and 4, respectively). These smaller polypeptide fragments still reacted with anti-D5/58-78, but were no longer reactive with antibody to D5/82-102 (Fig. 7,

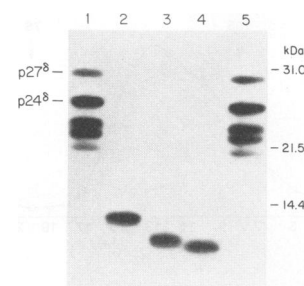


FIG. 6. Immunoblot analysis of chymotrypsin-digested HDaG. Chymotrypsin-digested liver-derived HDaG was separated by SDS-15% PAGE and transferred to Immobilon-p transfer membranes for detection of HDaG with guinea pig anti-D5/58-78 antibody. HDaG was digested for 30 min at 37°C at a chymotrypsin concentration of 0.5 µg/ml (lane 1), 5.0 µg/ml (lane 2), 50 µg/ml (lane 3), or 500 µg/ml (lane 4). Undigested antigen is shown in lane 5.

compare lanes A1 and B1 in panels b and c). Thus, these small digestion products do not contain an epitope representing residues 81 to 86, the minimum peptide segment located at the amino end of the peptide sequences recognized by the guinea pig anti-D5/82-102 in PEPSCAN analysis of hexamer peptides (Fig. 8). From these data, it can be deduced that the carboxy termini of the 10.0- and 10.5-kDa polypeptides do not extend beyond residue 85. Similar PEPSCAN analysis of guinea pig anti-D5/58-78 suggested that the carboxy termini of these chymotrypsin digestion fragments both extend beyond residue 68, as the hexapeptide 64 to 69 is the minimal amino-terminal peptide segment recognized by anti-D5/58-78 (Fig. 8). Between residues 69 and 85, possible chymotrypsin cleavage sites (at these high protease concentrations) include leucine, isoleucine, or methionine residues at positions 74, 76, 79, and 81 (Fig. 8). These results are thus consistent with the carboxy terminus of the 10.0-kDa peptide being located between Leu-74 and Met-79, and that of the 10.5-kDa molecule being located between Met-76 and Ile-81. The carboxy terminus of the 12.5 kDa fragment is likely to be at Phe-94 or Leu-90. Because antibody to a peptide representing the extreme amino terminus of HDaG (anti-D5/2-17) does not react with native or denatured HDaG (23), it was not possible to similarly map the amino termini of these digestion products. However, the apparent molecular masses of these polypeptide fragments suggested that the amino terminus of each was at or near the amino terminus of the full-length HDaG molecule.

Because the 10.0- and 10.5-kDa chymotrypsin digestion products contain a leucine zipper-like motif present between residues 27 and 58 of the intact protein (8), we were interested in determining whether either of these small HDaG fragments was capable of forming specific dimers. A crude liver extract containing HDaG was thus digested with chymotrypsin at concentrations of 500, 50, and 5 µg/ml. The products of each chymotrypsin digestion reaction were treated with 0.4% glutaraldehyde and then subjected to SDS-PAGE and immunoblotting against human polyclonal anti-HDV (Fig. 7a), guinea pig anti-D5/58-78 (Fig. 7b), or guinea pig anti-D5/82-102 (Fig. 7c). The concentration of protein in the liver extract was slightly higher than that in the digestion experiment shown in Fig. 6. However, as before, only the 10.0-kDa fragment was detected by polyclonal human convalescent antibodies after digestion with 500 µg of chymotrypsin per ml (Fig. 7a, lane A1). This product was no longer detectable after glutaraldehyde treatment (Fig. 7a,

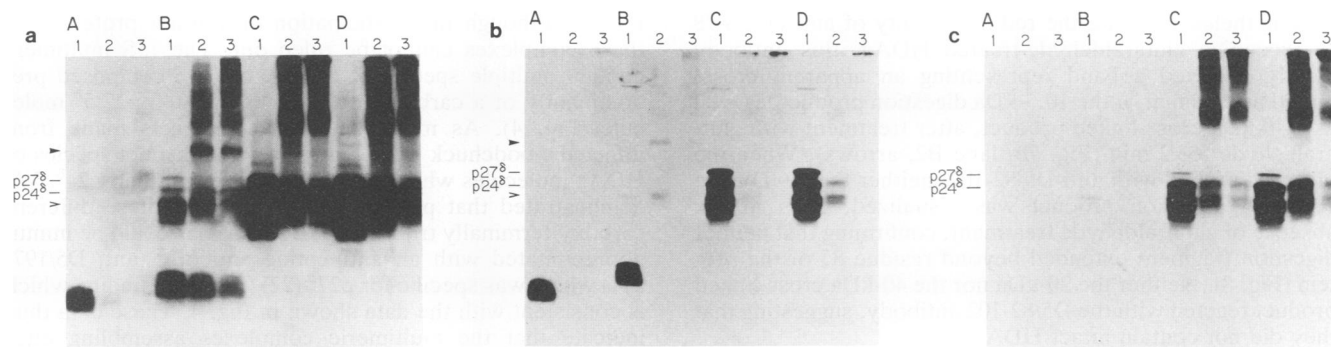


FIG. 7. Dimerization of chymotrypsin-digested HDAg, demonstrated by glutaraldehyde cross-linkage and then SDS-PAGE and immunoblot detection of antigen with polyclonal human antibody (a), guinea pig anti-D5/58-78 (b), or guinea pig anti-D5/82-102 (c). Liver-derived HDAG was digested for 30 min at 37°C with chymotrypsin at a concentration of 500 μ g/ml (lanes A1 to A3), 50 μ g/ml (lanes B1 to B3), or 5 μ g/ml (lanes C1 to C3). Nondigested HDAG is shown in lanes D1 to D3. Proteins present in aliquots of each protease digestion reaction and in the nondigested liver extract were cross-linked in the presence of 0.4% glutaraldehyde for 2 min (lanes 2) or 5 min (lanes 3). The material in all lanes 1 was not cross-linked with glutaraldehyde. Products were separated by SDS-15% PAGE, transferred to Immobilon-p transfer membranes, and probed with the indicated antibodies. Final detection of peroxidase-conjugated antibody was by the enhanced chemiluminescence system. Panels a and c represent the same blot, with panel c probed after removal of the antibody shown in panel a, as described in Materials and Methods.

lanes A2 and A3), suggesting that the epitopes present in this polypeptide fragment were destroyed by glutaraldehyde (see below). With a lesser concentration of chymotrypsin (50 μ g/ml), digestion was incomplete but resulted in substantial amounts of the 10.5-kDa product (Fig. 7a, lane B1). This product was diminished in quantity after glutaraldehyde treatment for 2 min, in association with the appearance of a new HDAG band of approximately 40 kDa (Fig. 7a, lane B2). This band was not present in lanes containing cross-linked HDAG which had not been digested with chymotrypsin (Fig. 7a, lanes D2 and D3), suggesting that it contained cross-linked forms of the 10.5-kDa digestion product (Fig. 7a, lane B1).

Because these cross-linking experiments were done with nonpurified liver extracts, the discrete size of the cross-linked 40-kDa product indicated that the HDAG digestion product was cross-linked to a specific molecule(s). The

apparent mass of the cross-linked complex (40 kDa) was inconsistent with formation of a simple dimer of the 10.5-kDa fragment and suggested that it might be a heterodimer or larger HDAG multimer. The possibility that cross-linked homodimers of the 10.5-kDa fragment were present but migrating at approximately the same rate as residual undigested HDAG could not be excluded. Longer exposure of the 50- μ g/ml chymotrypsin digestion product to glutaraldehyde (5 min, Fig. 7a, lane B3) resulted in further reduction of the amount of the 10.5-kDa product, as well as of the cross-linked 40-kDa product, and corresponding increases in yet higher-molecular-weight cross-linked HDAG complexes. In view of the fact that the carboxy terminus of the 10.5-kDa chymotrypsin digestion fragment is likely to terminate between residues 76 and 81 (Fig. 8), these data suggest that a dimerization domain exists within the amino-terminal 81 residues of HDAG.

To confirm the identity of the 10.0- and 10.5-kDa peptide fragments, a blot identical to that shown in Fig. 7a was probed with guinea pig antibodies to peptide D5/58-78 (Fig. 7b), while the blot shown in Fig. 7a was stripped of antibody and reprobed with guinea pig antibody to peptide D5/82-102 (Fig. 7c). These antipeptide antibodies demonstrated substantially less sensitivity for the detection of larger forms of HDAG (including p24⁸ and p27⁸) than the polyclonal antibody shown in Fig. 7a. This difference is compatible with our previous observations that the immunodominant epitopes recognized by polyclonal antisera lie between residues 156 and 184 of the molecule (23). Nonetheless, anti-D5/58-78 recognized both non-cross-linked 10.0- and 10.5-kDa fragments (Fig. 7b, lanes A1 and B1). The reactivity of the D5/58-78 antibody was markedly reduced after only 2 min of exposure of HDAG to glutaraldehyde. This reduction in antigenicity occurred even with HDAG which had not been digested with chymotrypsin and which was not cross-linked by this brief glutaraldehyde treatment (compare the relative intensities of p24⁸ bands in lanes C2 and D2 of Fig. 7b with the comparable lanes in Fig. 7a). Thus, glutaraldehyde treatment substantially damaged the major epitopes recognized by this antipeptide antibody (residues 64 to 73, Fig. 8).

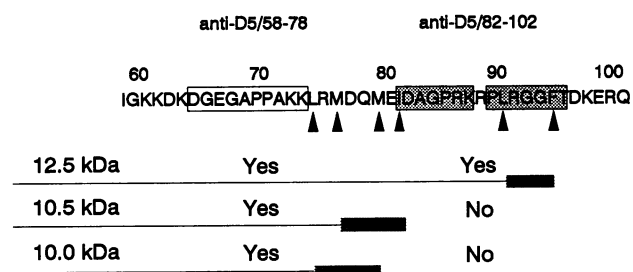


FIG. 8. Map showing epitopes recognized by guinea pig antibodies to peptides D5/58-78 and D5/82-102, as determined by their reactivity with hexapeptides synthesized on polyethylene pins (PEPSCAN analysis) (23). The open box indicates nested hexamer oligopeptide sequences recognized by anti-D5/58-78, while the shaded boxes represent hexapeptides recognized by anti-D5/82-102. Arrows indicate positions of residues with bulky side chains that represent potential chymotrypsin cleavage sites; stippled area represent the limits of the probable carboxy termini of the digestion products present in Fig. 6. The reactivity of the digestion products with the two peptide antibodies is summarized in the lower part of the figure.

Nonetheless, despite the reduced ability of anti-D5/58-78 to recognize glutaraldehyde-treated HDAg, this antibody clearly detected a band representing an apparent cross-linked homodimer of the 10.5-kDa digestion product, as well as a 40-kDa cross-linked product, after treatment with glutaraldehyde for 2 min (Fig. 7b, lane B2, arrows). When the blot was probed with anti-D5/82-102, neither the 10- nor the 10.5-kDa digestion product was visualized, even in the absence of glutaraldehyde treatment, confirming that neither digestion fragment extended beyond residue 85 of the protein (Fig. 8). Neither the 20-kDa nor the 40-kDa cross-linked product reacted with the D5/82-102 antibody, suggesting that they did not contain intact HDAg.

DISCUSSION

The p24^b and p27^b forms of HDAg are expressed from a single reading frame within the HDV genome, the only reading frame which is apparently expressed during replication of this unique animal virus. These proteins play important and strikingly different roles in the replication of the virus, with p24^b required for transport of the viral RNA to the nucleus, where it undergoes replication, and p27^b both acting as a dominant negative regulator of RNA replication and playing a key role in the assembly of HDV particles (3, 5, 21). In addition, while only p24^b and p27^b are detectable in serum, multiple smaller HDAg species are found in the liver of HDV-infected woodchucks. These smaller HDAg molecules are carboxy-terminally truncated forms of the protein, the smallest of which terminates between residues 130 and 160 (22). Recent evidence from our laboratory indicates that these are degradation products of p27^b or p24^b (2a). Their role, if any, in replication of the virus remains obscure.

Previous studies examining the stoichiometry of the dominant negative regulatory effects of p27^b on RNA replication suggested that p27^b may function as part of a multimeric HDAg complex (5). Other investigators have shown that segments of HDAg translated *in vitro* from recombinant cDNA form dimers (8). In addition, Macnaughton et al. (11) demonstrated large multimeric aggregates of HDAg (approximately 50S) in a stably transfected hepatoma-derived cell line expressing the small form of the antigen. In this report, we demonstrate by glutaraldehyde cross-linking that HDAg is naturally present as dimers *in vivo*. We showed that HDAg dimers are present in HDV particles circulating in the serum, as well as in HDAg extracted under denaturing conditions from the liver and subsequently renatured by dialysis against a nondenaturing buffer. Moreover, we demonstrated that large, multimeric complexes involving multiple copies of HDAg proteins are present in this dialyzed liver extract. These 15S complexes are associated with an as yet poorly characterized RNA that hybridizes with an antigenomic-sense RNA probe. The absence of a detectable band in attempts at Northern analysis (data not shown) and the more intense hybridization signal evident in fractions containing somewhat more rapidly sedimentary complexes (compare fractions 9 to 11 with 13 to 15 in Fig. 3A and 5) suggest that this RNA may be heterogeneous in size. Furthermore, the fact that the sedimentation rate of the 15S complexes fell to only 12S with digestion of the RNA suggests that the associated RNA is very likely to be subgenomic in size.

The HDAg multimers assembled with removal of guanidine from the liver extract. Analysis of the proteins present in various fractions from sucrose gradients containing these multimers indicated that they are specific aggregates of

HDAg, although the participation of another protein(s) in these complexes cannot be ruled out. The 15S multimers contain multiple species of HDAg, but are composed predominantly of a carboxy-terminally truncated p22.5^b molecule (Fig. 4). As mentioned above, extracts made from infected woodchuck liver contain several distinct species of HDAg molecules which are shorter in length than p24^b. We demonstrated that p24^b as well as each of these different carboxy-terminally truncated HDAg species could be immunoprecipitated with an antipeptide antibody (anti D5/197-211) which was specific for p27^b (22) (Fig. 1), a finding which is consistent with the data shown in Fig. 4. These data thus indicate that the multimeric complexes assembling after removal of guanidine are each composed of molecules of heterogeneous sizes. The apparent size of the smallest of these HDAg species suggests that the oligomerization domains responsible for formation of these complexes are located within the amino-terminal 130 to 160 residues of the protein (22). This finding is compatible with the lack of a role for disulfide bonds involving the conserved Cys-211 residue in formation of either dimers or multimers.

A small, 10.5-kDa polypeptide fragment produced by extensive chymotrypsin digestion of liver-derived HDAg and consisting of most if not all of the amino-terminal 81 residues of the protein retained the ability to form specific dimers (Fig. 7). This observation is consistent with the role proposed for a conserved leucine zipper-like motif located between residues 27 and 58, which has been suggested to be a possible dimerization domain (8). This domain contains a 3-4 hydrophobic residue repeat pattern, with hydrophobic residues (mostly leucine and isoleucine) occurring at alternating third and fourth residues (positions a and d) through a conserved series of three heptad repeats (Fig. 9). This sequence motif suggests that this region of HDAg forms a short, parallel coiled coil, similar to the dimerization domains of leucine zippers in the bZIP class of DNA-binding proteins (16). Consistent with this model of the HDAg dimerization domain, residues of opposing polarities are present at positions e and g within adjacent heptads, allowing for the presence of accessory electrostatic interactions between these residues which would serve to stabilize the hydrophobic interactions holding the two α -helices within the parallel coiled-coil structure (Fig. 9).

There are, however, some interesting and novel features to this proposed dimerization domain. The conserved Asn-Pro dipeptide sequence occurring at residues 48 and 49 would be predicted to possibly either break the α -helix or induce a bend in the α carbon chain. This is followed in the primary sequence by an additional 1.5 heptads containing a 3-4 hydrophobic repeat in the d and g positions (Fig. 9). Because at least 4 heptad repeats are usually required for a strong dimerization interaction in parallel coiled coils (16), it is possible that these additional 1.5 heptads participate in the dimerization interface. However, the structural impact of the conserved Pro-49 residue and the subsequent stutter in the series of 3-4 heptad repeats is uncertain. Interestingly, similar carboxy-terminal stutters (without a preceding Pro residue) have been noted in the much longer coiled-coil dimerization domains of the reovirus cell attachment protein, $\sigma 1$ (15).

The data presented in Fig. 6 suggest that the sensitivity of HDAg to cleavage by chymotrypsin is greatest in the middle and carboxy-terminal regions of HDAg and that the amino-terminal 75 to 81 residues are relatively resistant to the protease. This finding is consistent with a multimeric structure in which the amino-terminal third of the protein is

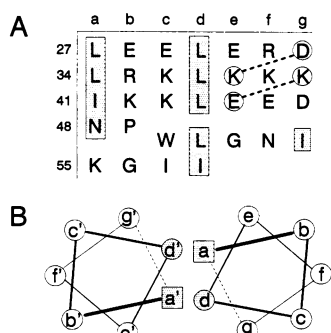


FIG. 9. Proposed parallel coiled-coil dimerization interface of HDAG molecules. (A) Conserved 3-4 hydrophobic repeat pattern present between residues 27 and 58. Each row represents one heptad, with residue positions within the heptads labelled a to g. To the left is the residue number (from the amino terminus of HDAG) of the first residue in each heptad. Hydrophobic residues interacting with their opposite member in the putative coiled coil are shown in shaded boxes (positions a and d before the stutter at Pro-49, and positions d and g thereafter). Residues with opposing charges in positions e and g in adjacent heptads before the stutter are circled and connected with dotted lines. The stutter at Pro-49 is represented as a downward shift in the sequence of the fourth heptad. (B) Orientation of the two helices within the parallel coiled-coil dimerization domain preceding the stutter. The view is from the amino end of the helices looking downward toward the carboxy end. The helices are held as dimers through hydrophobic interactions between residues at a and d, while electrostatic interactions between g' and e and e' and g provide additional stabilizing forces (16).

oriented toward the interior, with the carboxy-terminal regions of the protein oriented toward the exterior of the complex and thus more accessible to the protease. Such a hypothetical structure could also explain the relative lack of antigenicity of the amino terminus of the protein that we (22) as well as Bergmann and associates (1) have noted previously. Alternatively, it may be that the involvement of the coiled-coil domain (residues 28 to 58) within the dimerization interface protects this region of the protein from protease-mediated cleavage.

The fact that dimers of HDAG are found within circulating HDV particles (Fig. 2) indicates that dimerization is likely to play an important role in particle assembly. It is also possible that dimerization of the protein is required for interaction with the viral RNA, as has been shown to be the case with numerous nucleic acid-binding proteins. If this is the case, however, the orientation of the dimerization domain (residues 27 to 58) and the RNA-binding domain located between residues 79 to 163 (9) is reversed from that of the bZIP proteins, in which the DNA-binding domain is on the amino side of the coiled coil. However, the function of the multimeric aggregates identified within the infected woodchuck liver extract is unknown. Thus far, we have been unable to positively confirm the presence in HDV particles of HDAG multimers which are stable in the presence of 1.2% NP-40 (as are the multimers we have identified in the dialyzed liver extract) (unpublished data). Thus, the involvement of these multimers in particle assembly is uncertain. An alternative role in replication or transport of viral RNA remains possible, particularly in view of the possible association of the complexes with genomic-sense RNA.

ACKNOWLEDGMENTS

This work was supported in part by Public Health Service grant R01-HL37974.

We thank Paul Becherer for providing the pGEM[®] plasmid, Bruce Erickson and John Newbold for helpful discussions and review of the manuscript, and John Cullen for assistance in the production of antipeptide antibodies. We thank Skippy Hildebrants for assistance in preparation of the manuscript.

REFERENCES

- Bergmann, K. F., P. J. Cote, A. Moriarty, and J. L. Gerin. 1989. Hepatitis delta antigen: antigenic structure and humoral immune response. *J. Immunol.* **143**:3714-3721.
- Bergmann, K. F., and J. L. Gerin. 1986. Antigens of hepatitis delta virus in the liver and serum of humans and animals. *J. Infect. Dis.* **154**:702-706.
- Brown, E. A. Unpublished observations.
- Chang, F.-L., P.-J. Chen, S.-J. Tu, C.-J. Wang, and D.-S. Chen. 1991. The large form of hepatitis delta antigen is crucial for assembly of hepatitis delta virus. *Proc. Natl. Acad. Sci. USA* **88**:8490-8494.
- Chang, M.-F., S. C. Baker, L. H. Soe, T. Kamahora, J. G. Keck, S. Makino, S. Govindarajan, and M. M. C. Lai. 1988. Human hepatitis delta antigen is a nuclear phosphoprotein with RNA-binding activity. *J. Virol.* **62**:2403-2410.
- Chao, M., S.-Y. Hsieh, and J. Taylor. 1990. Role of two forms of hepatitis delta virus antigen: evidence for a mechanism of self-limiting genome replication. *J. Virol.* **64**:5066-5069.
- Glenn, J. S., J. A. Watson, C. M. Havel, and J. M. White. 1992. Identification of a prenylation site in delta virus large antigen. *Science* **256**:1331-1333.
- Kuo, M. Y. P., J. D. Goldberg, L. Coates, W. S. Mason, J. L. Gerin, and J. Taylor. 1988. Molecular cloning of hepatitis delta virus RNA from an infected woodchuck liver: sequence, structure, and applications. *J. Virol.* **62**:1855-1862.
- Lai, M. M. C., Y.-C. Chao, M.-F. Chang, J.-H. Lin, and I. Gust. 1991. Functional studies of hepatitis delta antigen and delta virus RNA, p. 283-292. In J. L. Gerin, R. H. Purcell, and M. Rizzetto (ed.), *The hepatitis delta virus*. John Wiley & Sons, Inc., New York.
- Lin, J.-H., M.-F. Chang, S. C. Baker, S. Govindarajan, and M. M. C. Lai. 1990. Characterization of hepatitis delta antigen: specific binding to hepatitis delta virus RNA. *J. Virol.* **64**:4051-4058.
- Luo, G., M. Chao, S.-Y. Hsieh, C. Sureau, K. Nishikura, and J. Taylor. 1990. A specific base transition occurs on replicating hepatitis delta virus RNA. *J. Virol.* **64**:1021-1027.
- Macnaughton, T. B., E. J. Gowans, B. Reinboth, A. R. Jilbert, and C. J. Burrell. 1990. Stable expression of hepatitis delta antigen in a eucaryotic cell line. *J. Gen. Virol.* **71**:1339-1345.
- Makino, S., M.-F. Chang, C.-K. Shieh, T. Kamahora, D. M. Vannier, S. Govindarajan, and M. M. C. Lai. 1987. Molecular cloning and sequencing of a human hepatitis delta (δ) virus RNA. *Nature (London)* **329**:343-346.
- Negro, F., K. F. Bergmann, B. M. Baroudy, W. C. Satterfield, H. Popper, R. H. Purcell, and J. L. Gerin. 1988. Chronic hepatitis D virus (HDV) infection in hepatitis B virus carrier chimpanzees experimentally superinfected with HDV. *J. Infect. Dis.* **158**:151-159.
- Negro, F., B. E. Korba, B. Forzani, B. M. Baroudy, T. L. Brown, J. L. Gerin, and A. Ponzetto. 1989. Hepatitis delta virus (HDV) and woodchuck hepatitis virus (WHV) nucleic acids in tissues of HDV-infected chronic WHV carrier woodchucks. *J. Virol.* **63**:1612-1618.
- Nibert, M. L., T. S. Dermody, and B. N. Fields. 1990. Structure of the retrovirus cell-attachment protein: a model for the domain organization of σ1. *J. Virol.* **64**:2976-2989.
- O'Shea E. K., J. D. Klemm, P. S. Kim, and T. Alber. 1991. X-ray structure of the GCN4 leucine zipper, a two-stranded, parallel coiled coil. *Science* **254**:539-544.
- Ponzetto, A., P. J. Cote, H. Popper, B. H. Boyer, W. T. London, E. C. Ford, F. Bonino, R. H. Purcell, and J. L. Gerin. 1984. Transmission of hepatitis B-associated delta agent to the eastern

- woodchuck. *Proc. Natl. Acad. Sci. USA* **81**:2208–2211.
18. **Rizzetto, M., B. Hoyer, M. G. Canese, J. W.-K. Shih, R. H. Purcell, and J. L. Gerin.** 1980. δ agent: association of δ antigen with hepatitis B surface antigen and RNA in serum of δ -infected chimpanzees. *Proc. Natl. Acad. Sci. USA* **77**:6124–6128.
 19. **Rizzetto, M., J. W.-K. Shih, and J. L. Gerin.** 1980. The hepatitis B virus-associated δ antigen: isolation from liver, development of solid-phase radioimmunoassays for δ antigen and anti- δ , and partial characterization of δ antigen. *J. Immunol.* **125**:318–324.
 20. **Ryu, W.-S., M. Bater, and J. Taylor.** 1992. Assembly of hepatitis delta virus particles. *J. Virol.* **66**:2310–2315.
 21. **Taylor, J. M.** 1990. Hepatitis delta virus: cis and trans functions required for replication. *Cell* **61**:371–373.
 22. **Wang, J.-G., J. Cullen, and S. M. Lemon.** 1992. Immunoblot analysis demonstrates that the large and small forms of hepatitis delta virus antigen have different C-terminal amino acid sequence. *J. Gen. Virol.* **73**:183–188.
 23. **Wang, J.-G., R. W. Jansen, E. A. Brown, and S. M. Lemon.** 1990. Immunogenic domains of hepatitis delta virus antigen: peptide mapping of epitopes recognized by human and woodchuck antibodies. *J. Virol.* **64**:1108–1116.
 24. **Wang, K.-S., Q.-L. Choo, A. J. Weiner, J.-H. Ou, R. C. Najarian, R. M. Thayer, G. T. Mullenbach, K. J. Denniston, J. L. Gerin, and M. Houghton.** 1986. Structure, sequence and expression of the hepatitis delta (δ) viral genome. *Nature (London)* **323**:508–514.
 25. **Wang, K.-S., Q.-L. Choo, A. J. Weiner, J.-H. Ou, R. C. Najarian, R. M. Thayer, G. T. Mullenbach, K. J. Denniston, J. L. Gerin, and M. Houghton.** 1987. Corrigendum: structure, sequence and expression of the hepatitis delta (δ) viral genome. *Nature (London)* **328**:456.
 26. **Weiner, A. J., Q.-L. Choo, K.-S. Wang, S. Govindarajan, A. G. Redeker, J. L. Gerin, and M. Houghton.** 1988. A single antigenomic open reading frame of the hepatitis delta virus encodes the epitope(s) of both hepatitis delta antigen polypeptides p24^h and p27^h. *J. Virol.* **62**:594–599.
 27. **Xia, Y.-P., C.-T. Yeh, J.-H. Ou, and M. M. C. Lai.** 1992. Characterization of nuclear targeting signal of hepatitis delta antigen: nuclear transport as a protein complex. *J. Virol.* **66**:914–921.